CHAPTER TWELVE

Ductile Shear Zones, Textures, and Transposition

12.1 INTRODUCTION

Imagine a cold and wet day in northern Scotland, which is not a far stretch of the imagination if you've visited the area. While mapping part of the Scottish Highlands you are struck by the presence of highly deformed rocks that overlie relatively undeformed, flat-lying, fossiliferous sediments. This relationship is even more startling because the overlying unit has experienced much higher grade metamorphism than the underlying sediments, and it contains no fossils. When you arrive at the contact between these two rock suites, you notice that they are separated by a distinctive layer of light-colored, powdery-looking rock. The regional relationships of the suites and their superposition already suggest that the contact is a low-angle reverse (or, thrust) fault. So, what is the distinctive fine-grained rock at the contact? In your mind you envision the incredible forces associated with the emplacement of the hanging wall unit over the footwall, and you surmise that the rock at the contact was crushed and milled, like what happens when you rub two bricks against each other. Using your class in ancient Greek, you decide to coin the name **mylonite** for this fine-grained layer, because "mylos" is Greek for milling.

Something like this happened over a hundred years ago in Scotland where the late Precambrian Moine Series ("crystalline basement") overlie a Cambro-Ordovician quartzite and limestone ("platform") sequence along a Middle Paleozoic low-angle reverse fault zone, called the Moine Thrust. This classic Caledonian area was mapped by Charles Lapworth of the British Geological Survey in the late nineteenth century. Anecdote has it that Lapworth became convinced that the Moine Thrust was an active fault and that it would ultimately destroy his nearby cottage and maybe take his life; Lapworth's later years were spent in great emotional distress.

In most areas around the world you will find zones in which the deformation is markedly concentrated (Figure 12.1). Deformation in these zones is manifested by a variety of structures, which may include isoclinal folds, disrupted layering, and particularly well-developed foliations and lineations, among other deformation features. These zones, called ductile shear zones, often preserve crucial information about the tectonic history of an area, so they merit careful study. We begin their description with a definition. A **ductile shear zone** is a tabular band of definable width in which there is considerably higher strain than in the surrounding rock. The total strain within a shear zone typically has a large component of

(a)

(b)

FIGURE 12.1 (a) The Parry Sound shear zone in the Grenville Orogen (Ontario, Canada) displays characteristics that are common in ductile shear zones, including mylonitic foliation, mineral lineation (stretching lineation) and rotated clasts. (b) A close-up of the zone highlights the mylonitic foliation.

simple shear, where rocks on one side of the zone are displaced relative to those on the other side. In its most ideal form, a shear zone is bounded by two parallel boundaries, outside of which there is no strain. In real examples, however, shear zone boundaries are gradational. The adjective "ductile" is used because the strain accumulates by ductile processes, which can range from cataclasis to crystal-plasticity to diffusion (Chapter 9). So, a shear zone is like a fault in the sense that it accumulates relative displacement of rock bodies, but, unlike a fault, displacement in a ductile shear zone occurs by ductile deformation mechanisms and no throughgoing fracture is formed. This absence of a single fracture is a consequence of movement under relatively high temperature conditions or low strain rates, as we saw in the deformation experiments of Chapter 5.

Consider a major displacement zone that cuts through the crust and breaches the surface (Figure 12.2). In the first few kilometers below Earth's surface, **brittle processes** occur along the discontinuity, which result in earthquakes if the frictional resistance on discreet fracture planes is overcome abruptly. Displacement may also occur by movement on many small fractures, a ductile process called *cataclastic flow* (Chapter 9). In either case, frictional processes dominate the deformation at upper levels of the discontinuity, and this crustal segment is, therefore, called the **frictional regime.** Mechanically, this region is pressure sensitive. With depth, crystal-plastic and diffusional processes, such as recrystallization and superplastic creep, become increasingly important, primarily because temperature increases. Where these mechanisms are dominant, typically below a depth of 10–15 km for normal geothermal gradients (20°C/km–30°C/km) in quartz-dominated rocks, we say that displacement on the discontinuity occurs in the **plastic regime.** Rather than being pressure sensitive, deformation in this region is mostly temperature sensitive. Not surprisingly, the transitional zone between a dominantly frictional and dominantly plastic regime is called the **frictional-plastic transition,** or, more commonly, the **brittle-plastic transition.**[1] While

[1]*Frictional-plastic transition* avoids confusion surrounding the terms brittle, ductile, and plastic (see Chapter 5), but brittle-ductile and brittle-plastic are more widely used synonyms.

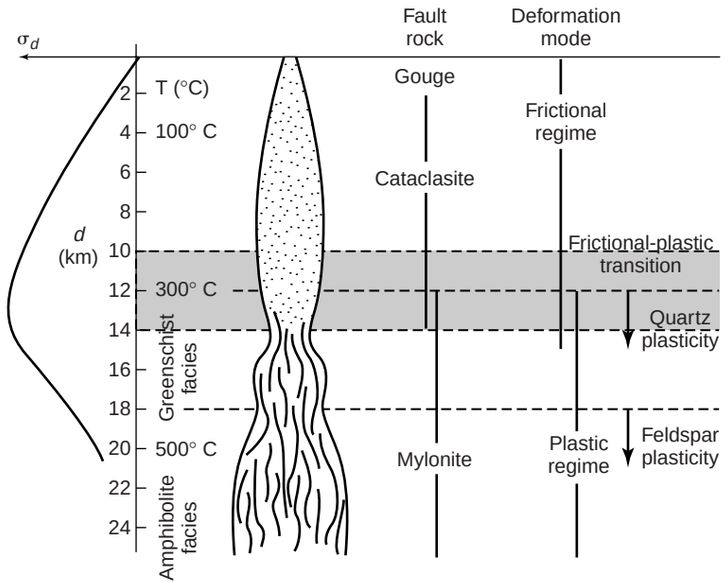

FIGURE 12.2 Integrated model for a displacement zone that cuts deep into the crust, showing the frictional and plastic regimes, the frictional–plastic transition, and crustal strength (σ_d); this is sometimes called the Sibson-Scholz fault model. Fault rocks typically found at crustal levels are indicated.

this term is in common use, it is technically not correct to call this the *brittle-ductile transition*, because ductile processes (such as cataclasis) may occur in the frictional regime. For example, we see that a crustal-scale displacement zone is a brittle fault at the surface and is a ductile shear zone at depth. Based on this contrast in deformation processes, we predict that the displacement zone will change from a relatively narrow fault zone to a broader ductile shear zone with increasing depth, because the strength contrast between deformation zone and host rock decreases.

Mylonites are dominated by the activity of crystal-plastic processes, which produce another characteristic of deformed rocks: **crystallographic-preferred fabrics** or **textures.** Textures are discussed in this chapter, although the topic logically follows the material on crystal-plasticity that is presented in Chapter 9. Secondly, rocks within ductile shear zones are typically intensely folded and the original layering is transposed into a tectonic foliation. A description of transposition will therefore close this chapter, but we emphasize that it is not unique to ductile shear zones (see also Chapter 11). We'll see that shear zones may produce more than one foliation and one or more lineations, and that shear-zone rocks commonly contain rotated fabric elements, grain-shape fabrics, and a grain size that is characteristically smaller than that of the host rock. Arguably, ductile shear zones are the most varied structural feature, and perhaps the most informative for tectonic analysis. Enough hype; let's look at these things.

12.2 MYLONITES

The inference made by Charles Lapworth concerning the formation of mylonites at the Moine Thrust is incomplete and, mechanically, incorrect. As mentioned earlier, the derivation of the name mylonite suggests that cataclastic flow is the process of grain-size reduction. In fact, microstructures in samples that record the change from relatively undeformed to mylonitized rock show that **crystal-plastic processes,** and **dynamic recrystallization** in particular, are mainly responsible for grain-size reduction (Figure 12.3). Therefore, we restrict the use of the term mylonite to a fault rock type with a relatively fine grain size as compared to the host rock and resulting from crystal-plastic processes. When brittle fracturing produces a reduced grain size, these fault rock types are called cataclasites. The field terminology of fault rocks and the processes by which they generally form are summarized in Table 12.1.

Mylonites are associated with all kinds of ductile shear zones, whether they result in reverse displacement (such as the Moine Thrust in Scotland), normal displacement (such as those in core complexes and the Basin-and-Range of the western USA), or strike-slip displacement (such as the Alpine fault in New Zealand). In each of these structural settings mylonites have one element in common: conditions that promote crystal-plastic deformation mechanisms. Such conditions are reached at various values of temperature, strain rate, and stress, depending on the dominant mineral in the rock (Chapter 9). For example, marble mylonites and quartzite mylonites form at temperatures that are lower than those under which feldspathic mylonites form, because the onset of dynamic recrystallization occurs at different temperatures in calcite (>250°C), quartz (>300°C), and feldspar (>450°C). Rocks that contain a variety of minerals show mixed behavior; for example, quartz grains in a sheared granite may dynamically recrystallize, while feldspar grains deform predominantly by fracturing. If the rock displays this contrast, we surmise that it was sheared at temperatures greater than 300°C, but less than 500°C (the greenschist facies of metamorphism). However, mylonite textures should not be used as a quantitative indicator of the conditions of temperature, stress, or

FIGURE 12.3 Clastomylonite containing relatively rigid clasts of varied lithologies in a fine-grained, crystal-plastically deformed marble matrix (Grenville Orogen, Ontario, Canada); hammer for scale.

TABLE 12.1	FAULT ROCKS AND PROCESSES
Breccia	Incohesive fault rock with randomly oriented fragments that make up >30% of the rock mass, formed by brittle processes. Because breccia is also a sedimentary rock, the adjective "tectonic" is often included for these fault rocks.
Cataclasite	Cohesive fault rock generally with randomly oriented fabric, formed by brittle processes.
Gouge	Fault rock formed under brittle conditions with randomly oriented fragments that make up <30% of the rock mass. Clay-rich gouge is typically more cohesive than clastic gouge, because of the presence of sticky, swellable clays.
Mylonite	Cohesive, foliated fault rock, formed dominantly by crystal-plastic processes.
Pseudotachylite	Dark, glassy fault rock along fractures, formed by melting of the host rock from heat generated during frictional sliding; they are likely associated with earthquake activity. *Note:* Tachylite is an old name for an igneous rock with a glassy texture.

strain rate, because of the uncertainties surrounding these parameters and their mutual dependence; at best we can make semiquantitative estimates such as those above. Quantitative metamorphic petrology and isotope geology, in many instances, provide reliable methods to determine the past conditions of temperature and pressure of deformed rocks (see Chapter 13), so we do not have to rely on microstructures only.

12.2.1 Types of Mylonites

The study of mylonites, which occur widespread in crustal rocks, has led to the development of several prefixes to distinguish among different types of mylonites. These terms are listed in Table 12.2.

Protomylonite and **ultramylonite** are used to describe mylonites in which the proportion of matrix is <50% and 90–100%, respectively. In a protomylonite, only part of the rock is mylonitized, whereas pervasive mylonitization has occurred in an ultramylonite. Mylonites containing 50–90% matrix are known simply as *mylonite*. **Blastomylonite** and **clastomylonite** are used to describe mylonites containing large grains surrounded by a fine-grained matrix that grew during mylonitization or that remained from the original rock, respectively. The terms derive from the Greek words "blastos," meaning growth and "klastos," meaning

TABLE 12.2	TYPES OF MYLONITES
Blastomylonite	Mylonite that contains relatively large grains that grew during mylonitization (e.g., from metamorphic reactions or secondary grain growth).
Clastomylonite	Mylonite that contains relatively large grains or aggregates that remain after mylonitization reduced the grain size of most of the host rock (e.g., relatively undeformed feldspar grains or clumps of mafic minerals).
Phyllonite	Mica-rich mylonite.
Protomylonite	Mylonite in which the proportion of matrix is <50% (i.e., rocks in which only a minor portion of the minerals underwent grain-size reduction).
Ultramylonite	Mylonite in which the proportion of matrix is 90–100% (i.e., rocks in which mylonitization was nearly complete).

broken. These prefixes are used for microstructural description of mylonites, but they are also used as field terms. Clastomylonite is used to describe mylonites that contain coarse fragments of less deformed host rock or exotic lithologies; for example, mafic clasts in a marble mylonite (Figure 12.3).

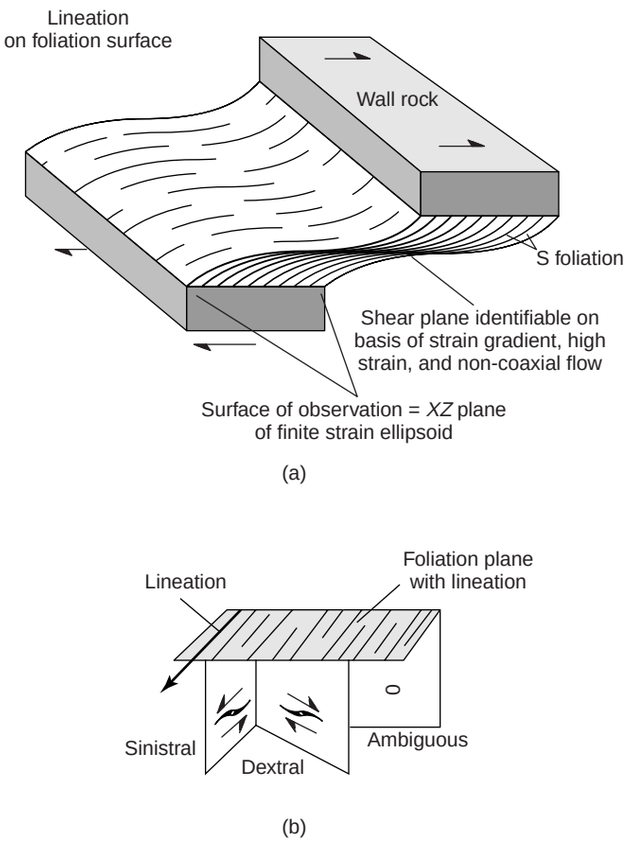

FIGURE 12.4 (a) Schematic, right-lateral ductile shear zone showing mylonitic foliation (S) and lineation. The optimal surface for study is the *XZ*-plane of the finite strain ellipsoid. (b) Apparent difference in shear sense, which results from observing the shear-sense indicator in different surfaces. Note that the surface perpendicular to the lineation and the foliation gives no shear-sense information.

12.3 SHEAR-SENSE INDICATORS

Ductile shear zones concentrate displacement at deeper levels in the crust, where recognizable markers that determine offset, such as bedding, are often absent. Consider a greenschist-facies shear zone in a large granitic body. The granitic rocks on either side of the mylonite are indistinguishable, so there is nothing at first glance to predict the sense of displacement, let alone the magnitude of displacement. **Sense of displacement** describes the relative motion of opposite sides of the zone (left-lateral or right-lateral, up or down, and so on), whereas **magnitude of displacement** is the distance over which one side moves relative to the other. The solution to this challenge is to look for **shear-sense indicators**[2] in ductile shear zones.

[2]The term *kinematic indicators* is often used as a synonym, but this suggests information about the strain state rather than sense of displacement.

12.3.1 Plane of Observation

The recognition and interpretation of shear-sense indicators require that we examine a shear zone in a particular orientation. Most mylonites contain at least one foliation and a lineation, which we use as an **internal reference frame.** In the field we look for outcrop surfaces (or cut an oriented sample in the lab) that are perpendicular to the mylonitic foliation and parallel to the lineation (Figure 12.4a). We make the reasonable assumption in this case that the lineation coincides with the movement direction of the shear zone. When two foliations are present, this surface is also generally perpendicular to their intersection. This plane, which parallels the *XZ*-plane of the finite strain ellipsoid, maximizes the expression of the rotational component of the deformation; in all other surfaces this compo-

nent is less. Then we must place the orientation of our surface in the context of the region. Say, we find that a right-lateral displacement is the surface of observation. Were we to look at this same surface from the opposite side, the displacement would appear to be left-lateral (Figure 12.4b). This is not a paradox, but simply a matter of reference frame; we encountered the same situation with fold vergence (Chapter 9). Because the displacement sense is the same in geographic coordinates, it is a good habit to analyze surfaces in the same orientation across the field area to avoid confusion. If this is not possible, make careful field notes of the orientation of the surface in which you determined shear sense. Back in the laboratory the rock saw offers complete control, provided you oriented the sample prior to removing it from the field. Having cautioned you sufficiently about orientation, let us now look at types of shear-sense indicators. They fall into five main groups: (1) grain-tail complexes, (2) disrupted grains, (3) foliations, (4) textures (or crystallographic fabrics), and (5) folds.

12.3.2 Grain-Tail Complexes

Mylonites commonly contain large grains or aggregates of grains that are surrounded by a finer matrix; for convenience, we use the term *grain* in a general sense to describe both large single grains and coherent grain aggregates. These grains may have *tails* of material with a composition and/or grain shape and size that differ from the matrix, such that they are distinguishable. For example, large feldspar grains connected by thin layers of finer-grained feldspathic material are common in gneiss (Figure 12.5). The tail may represent highly attenuated, preexisting mineral grains, it may be a consequence of dynamic recrystallization of material at the rim of the grain, or it may be material formed by synkinematic metamorphic reactions (neocrystallization). During deformation, the grains act as rigid bodies and we may be able to determine the sense of displacement from the tails. Based on their relationship with the shear-zone foliation, we recognize two types of grain-tail complexes: σ-type and δ-type. A third type, θ-complexes, has been proposed, but their interpretation is equivocal and we do not further discuss them.

Grain-tail complexes of the **σ-type** are characterized by wedge-shaped tails that do not cross the reference plane when tracing the tail away from the grain (Figure 12.6a). Sometimes the tail is flat at the top and the other side is curved toward the reference plane. Overall it has a stair-stepping geometry in the direction of displacement. This grain-tail geometry looks like the Greek letter σ (at least in the case of right-lateral displacement), hence the name σ-type. Figure 12.5a is a field example of a σ-type complex in a quartzofeldspathic shear zone. Obviously, in the case of left-lateral displacement the geometry is a mirror image.

In **δ-type** grain-tail complexes the tail wraps around the grain such that it cross cuts the reference plane when tracing the tail away from the grain (Figure 12.6b). If you rotate the Greek letter δ over 90° you will see why we use this symbol. Figure 12.5b is a field example of a δ-type complex in another feldspathic shear zone. The rotation on the δ-type complex is counterclockwise for left-handed and clockwise for right-handed displacement. The stair-stepping geometry that we find in σ-type grain-tail complexes is no longer a characteristic of displacement in δ-type complexes.

It is common to find both σ- and δ-types in one surface; even complexes that have characteristics of both σ- and δ-types may occur, because they are related (Figure 12.6c). One reason for this mixed occurrence is a varying relationship between the rate of recrystallization/neocrystallization and rotation of the grain. If tail formation is fast relative to rotation, the tails are of the σ-type. If, on the other hand, the rotation of the grain is faster, the tail will simply be dragged along and wrap around the grain (δ-type). The case of preexisting tails, which often occur with pegmatites that are incorporated into a shear zone, falls in the latter category.

The presence of both σ- and δ-type grain-tail complexes may indicate different rates of tail growth, different initial grain shape, different times of tail formation, or different coupling (see later section). From these variables it is clear that we should use grain-tail complexes with considerable caution for strain quantification purposes, but there is no doubt about their power as shear-sense indicators. In practice, geometries of the σ-type may be difficult to recognize, but δ-type complexes offer intuitively obvious and unequivocal information on shear sense.

12.3.3 Fractured Grains and Mica Fish

Minerals such as feldspar may deform by fracturing (Figure 12.7a) along crystallographic directions or parallel to the shortening direction (extension cracks). As long as the approximate orientation of these fractures before shear is known, we can determine the shear sense from their displacement (Figure 12.8). Fractures oriented at low angles to the mylonitic foliation have a

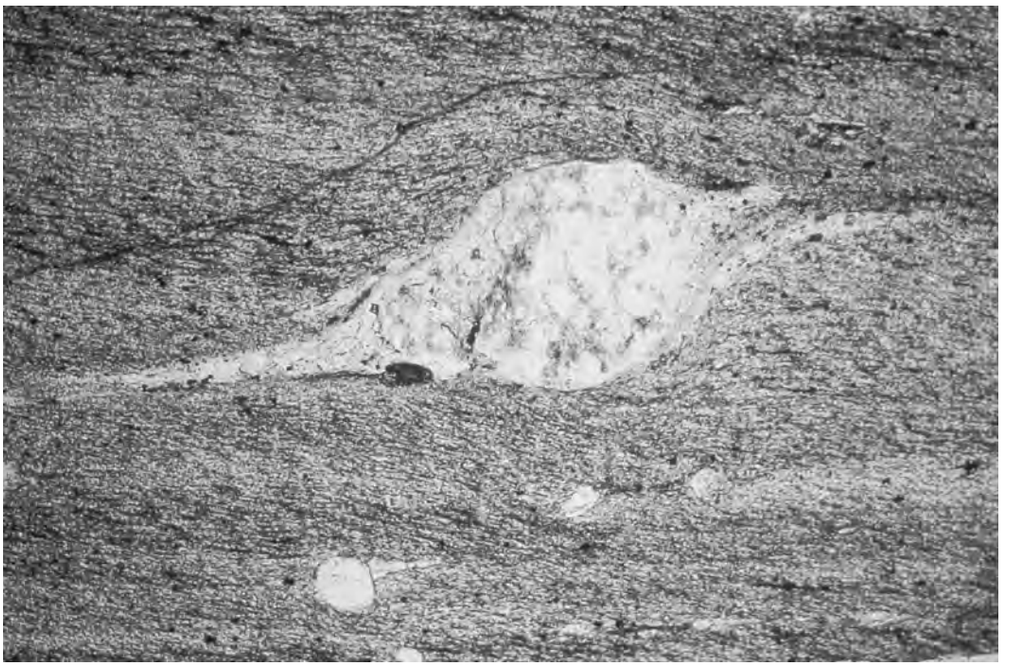

(a)

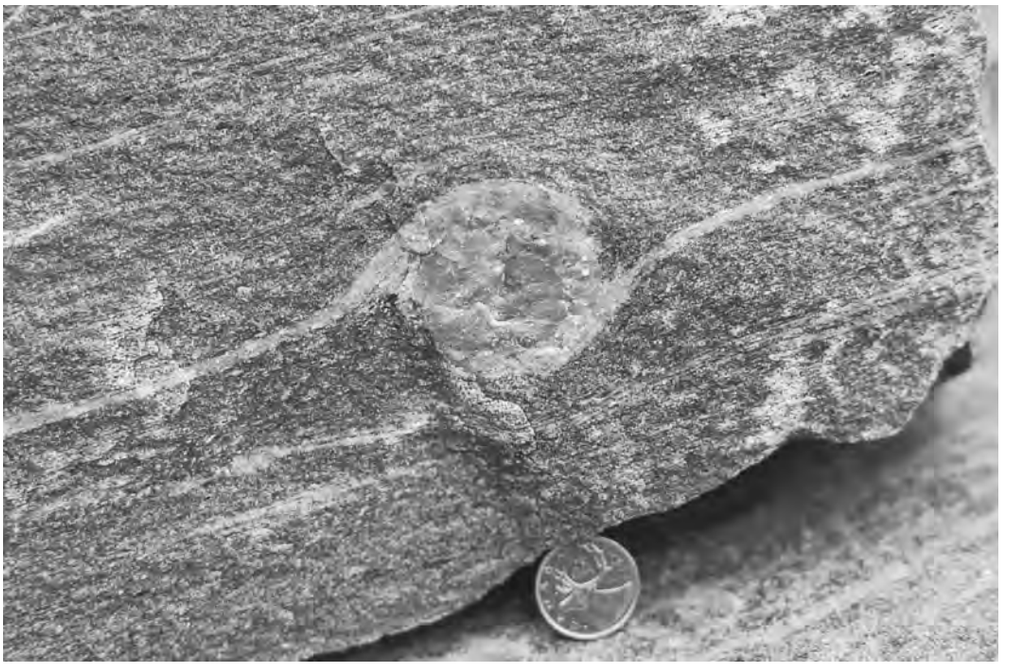

(b)

FIGURE 12.5 Grain-tail complexes. (a) A K-feldspar clast with a tail of fine-grained plagioclase of the σ-type complex (California, USA). (b) A δ-type complex in a feldspathic gneiss from the Parry Sound shear zone of the Grenville Orogen (Canada). Width of view is ~10 cm.

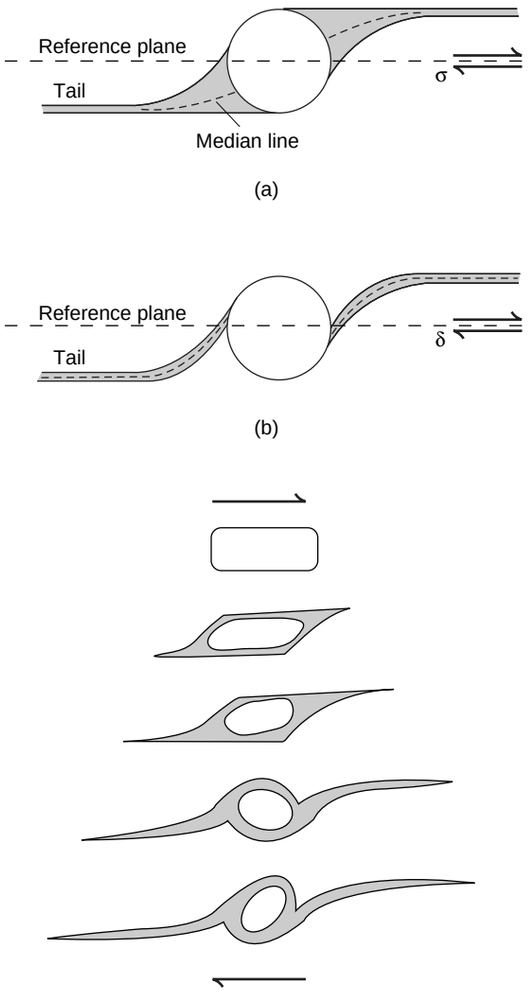

FIGURE 12.6 Grain-tail complexes as shear-sense indicators. (a) σ-type complex, (b) δ-type complex, and (c) the evolution of a σ-type complex into a δ-type grain-tail complex.

displacement sense that is consistent with the overall shear sense of the zone; these fractures are called **synthetic fractures** (Figure 12.8a). Fractures at angles greater than ~45° to the foliation show an opposite sense of movement; these are called **antithetic fractures** (Figure 12.8b). The opposite motion is not contradictory, as we can see from a simple experiment. Place a series of dominos upright between your hands, and move your hands in opposite directions. You will notice that as long as the angle of the dominos with your hands remains greater than ~45°, the displacement between individual dominos is opposite (antithetic) to the relative movement direction of your hands. At lower angles you will find that displacement of the dominos has a motion that is the same (synthetic) to the motion of your hands. Fractured minerals

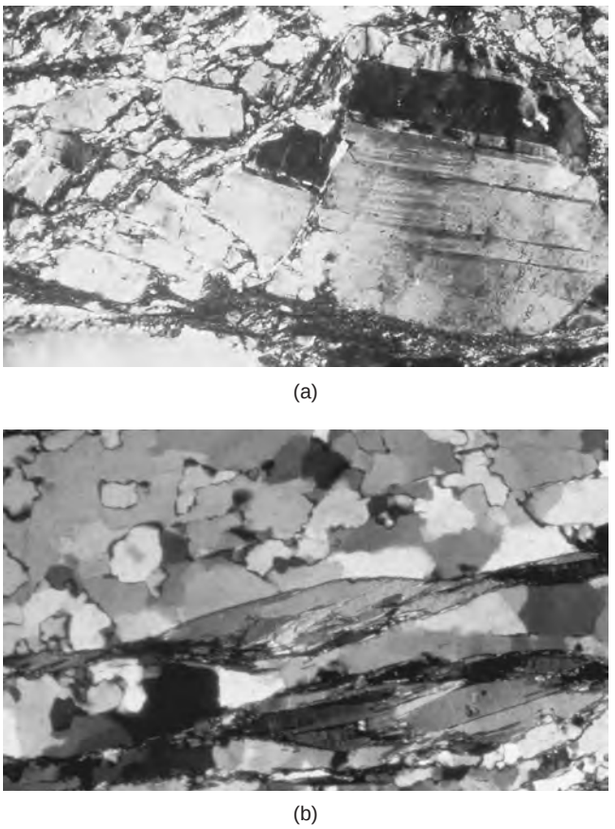

FIGURE 12.7 (a) Photomicrograph of fractured feldspar grain showing bookshelf- or domino-type, antithetic displacement. (b) Mica fish in a quartz mylonite. Right-lateral displacement in both images; width of view ~0.5 mm.

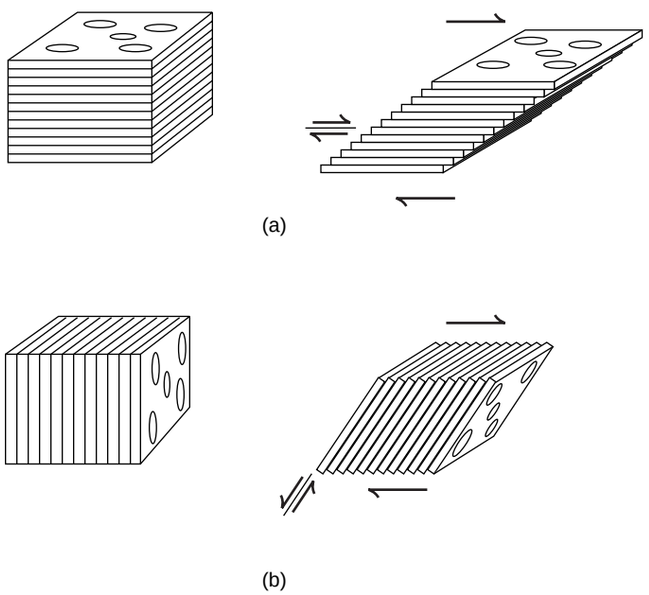

FIGURE 12.8 Placing dominos between a pair of hands to demonstrate sense of shear from fractured grains, if the fractures are at a low angle (a) or high angle (b) to the shear plane. Note that rotation according to the "domino model" of individual segments of fractured grains in (a) is the same as that for rotated grains.

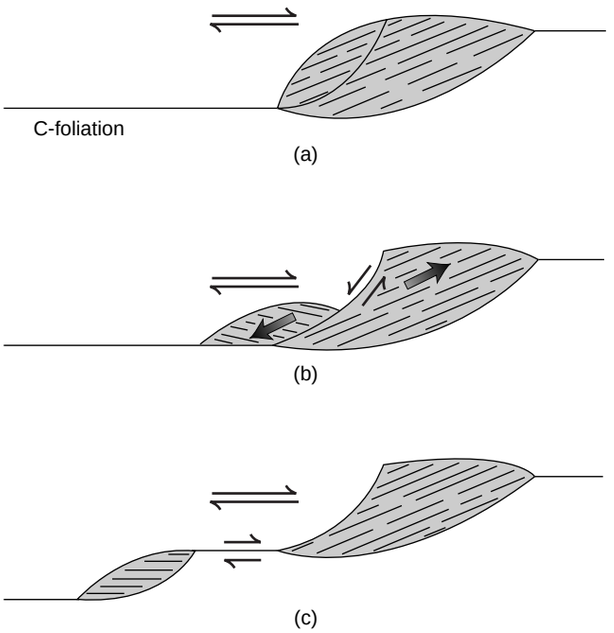

FIGURE 12.9 The formation of mica fish; (a) to (c) show successive stages in mica-fish development, with C-foliation marking the shear plane.

and clasts behave similarly in shear zones, and some therefore call this the *domino model*[3] for shear sense.

Feldspar and quartz are not the only minerals useful for determining shear-sense in mylonites. It is quite common to find large phyllosilicate grains, such as mica and biotite in quartzo-feldspathic rocks, and phlogopite in marbles, that display a characteristic geometry. The micas are connected by a mylonitic foliation, and their basal (0001) planes are typically oriented at an oblique angle to the mylonitic foliation, such that they point in the direction of the instantaneous elongation axis. In this orientation they show a stair-stepping geometry in the direction of shear (Figures 12.7b and 12.9), which is similar to σ-type grain-tail complexes that also step up in the shear direction. When phyllosilicates are large enough to be seen in hand specimens they look like scales on a fish (hence they are called **mica fish**) and you can use a simple field test to determine their approximate orientation. The basal planes of phyllosilicates are excellent reflectors of light, so when you turn the foliated shear-zone sample in the sun you encounter an orientation that is particularly reflective. When this happens and the sun is behind you, you are looking in the direction of shear. The method is affectionately known as the "fish flash," and was obviously developed by those fortunate geologists who work in sunnier parts of the world.[4]

12.3.4 Foliations: C-S and C-C′ Structures

Most mylonites show at least one well-developed foliation that is generally at a low angle to the boundary of the shear zone. Previously this foliation was called the **mylonitic foliation,** and it is otherwise known as the **S-foliation;** S is derived from the French word for foliation, "schistosité." Its angle with the shear zone boundary may be as little as a few degrees, at which point it is hard to distinguish from a foliation that parallels the shear zone boundary, called the **C-foliation;** C comes from "cisaillement," which is French for shear. A third foliation showing discrete shear displacements that is oblique to the shear zone boundary is called the **C′-foliation.** These are the three most

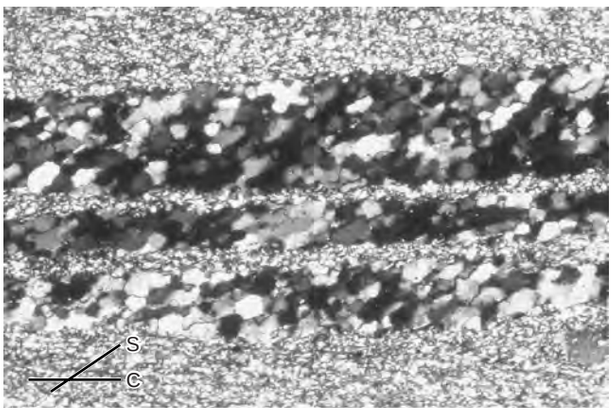

(a)

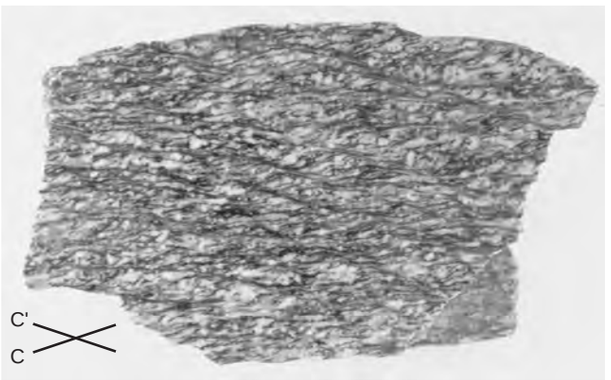

(b)

FIGURE 12.10 Photomicrograph of a C-S structure in a quartzite mylonite (a) and C-C′ structure in a micaceous mylonite (b); width of view is ~1 mm and ~15 cm, respectively.

[3]More literate, less playful geologists prefer the term *bookshelf model.*

[4]Less fortunate geologists resort to the fish flash*light* method.

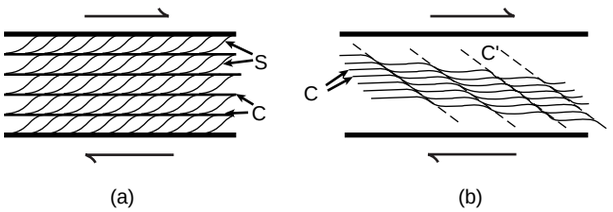

FIGURE 12.11 Characteristic geometry of (a) C-S and (b) C-C′ structures in a dextral shear zone. The C-surface is parallel to the shear zone boundary and is a surface of shear accumulation (i.e., not parallel to a plane of principal finite strain). The S-foliation is oblique to the shear-zone boundary and may approximate the *XY*-plane of the finite strain ellipsoid. The C′-foliation in (b) displaces an earlier foliation (C or composite C/S).

common foliations in shear zones and may reflect grain-shape fabrics or discrete shear surfaces. At first, these many foliations may seem confusing, but when correctly identified they become very powerful shear-sense indicators.

Thin-section study of well-developed mylonites in quartzites, granites, and marbles often shows the presence of a foliation that is defined by elongate grains (Figure 12.10a). This foliation reflects the activity of crystal-plastic processes that tend to elongate grains toward the extension axis of the finite strain ellipsoid, and is called the S-foliation. It is uncertain whether the S-foliation exactly tracks the *XY*-plane of the finite strain ellipsoid; nor is it certain whether S- and C-foliations form simultaneously or sequentially. These distinctions are only important when **C-S structures** are used to determine the degree of non-coaxiality or the kinematic viscosity number (Chapter 4). For their purpose as a shear-sense indicator, these questions are somewhat academic, because in all cases the geometry of a C-S structure gives the same shear sense. The long axis of elongate grains in the S-surface points up in the direction of shear, and the shear direction is perpendicular to the intersection line of the S- and C-foliations (Figure 12.11a).

Another common shear-sense indicator is a series of oblique, discrete shears that are present in strongly foliated mylonites. These small shears, called C′-surfaces because they accumulate shear strain, are particularly common in phyllosilicate-rich mylonites and crenulate or offset the mylonitic foliation (Figure 12.10b). C′-foliations are, therefore, also called **shear bands** or extensional crenulations. The offset on C′-surfaces is in the same direction as the overall displacement in the shear zone (i.e., displacement along C). The C′-surfaces contrast with S-surfaces that do not appear to displace the C-surface, suggesting that C′-surfaces form late in the mylonitic evolution. As with C-S structures, the strain significance of **C-C' structures** is incompletely understood, but their formation reflects a component of extension along the main anisotropy (the C-surface) of the mylonite. Thus, the shear sense on C-C′ structures is *synthetic* to the sense of shear of the zone as a whole (Figure 12.11b).

12.3.5 A Summary of Shear-Sense Indicators

Shear sense in ductile shear zones is only reliably determined when two or more different indicators give a consistent sense of displacement. So we close this section with a summary diagram (Figure 12.12) showing common shear-sense indicators that may be encountered in a ductile shear zone. Of all indicators, C-S and δ-clasts are most readily interpretable. Planar objects may have synthetic and antithetic shear, and C′ surfaces may reflect opposing motions; for example, boudins may show antithetic bookshelf faulting or synthetic displacement shear. The occurrence of a particular indicator will vary within a zone and even within the same outcrop, as a function of the dominance and

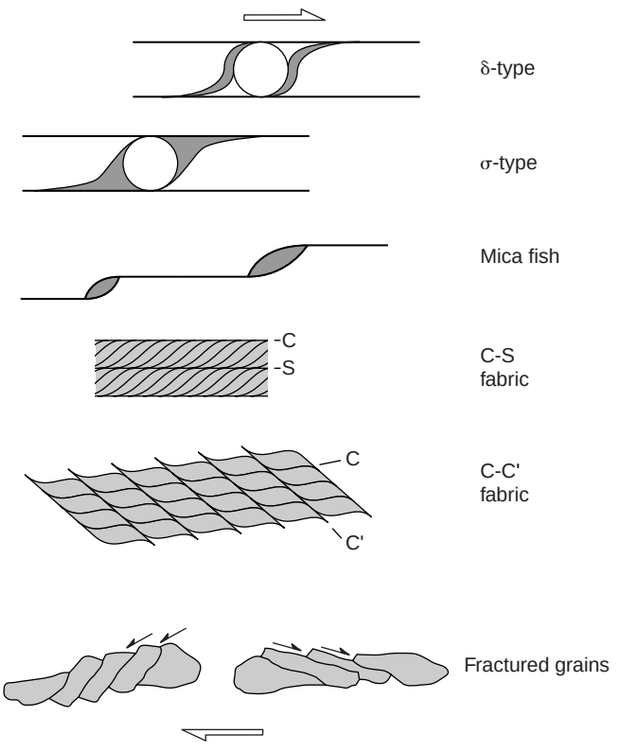

FIGURE 12.12 Summary diagram of shear-sense indicators in a dextral shear zone. A copy of this figure on a transparency (for left- and right-lateral shear) makes a handy inclusion in your field notebook.

mineralogy of grains and presence of foliations. Except for fractured grains, the shear sense can be determined from any of these indicators without knowing their (original) relationship to the shear-zone boundary. Figure 12.12 is another handy reference tool for your field notebook.

12.4 STRAIN IN SHEAR ZONES

In Chapter 4 we introduced a number of methods to quantify strain in deformed rocks, including the use of grain shapes. But do any of these methods apply to shear zones? Well, even if we accept that grain shape or degree of grain alignment reflects strain, at best we may be able to measure an incremental part of the strain history from the activity of dynamic recrystallization in mylonites. However, we have little or no idea how much of the finite strain this increment represents, nor to what extent the increment coincides with the orientation of the finite strain ellipsoid. Two approaches can be used to give at least a first-order estimate of the amount of finite strain in shear zones, namely, rotation of grains, and deflection of foliations; but, as you will see, these methods are not without their limitations. It is exactly because of the uncertainties surrounding strain analysis in shear zones that we have left a description of these methods until this chapter.

12.4.1 Rotated Grains

The formation of a ductile shear zone involves an internal rotation (the internal vorticity; Chapter 4) that may be recorded in rotated grains. So, from grains that preserve evidence of rotation we can determine this component of strain. We saw this earlier with δ-type grain-tail complexes, but this is also found in minerals that grow and incorporate matrix grains during rotation. In particular the mineral garnet shows this behavior, in which "trapped" matrix grains eventually produce a spiraling trail. Such garnets are often called **snowball garnets,** for obvious reasons (Figure 12.13). Let's use another simple analog experiment. Place a

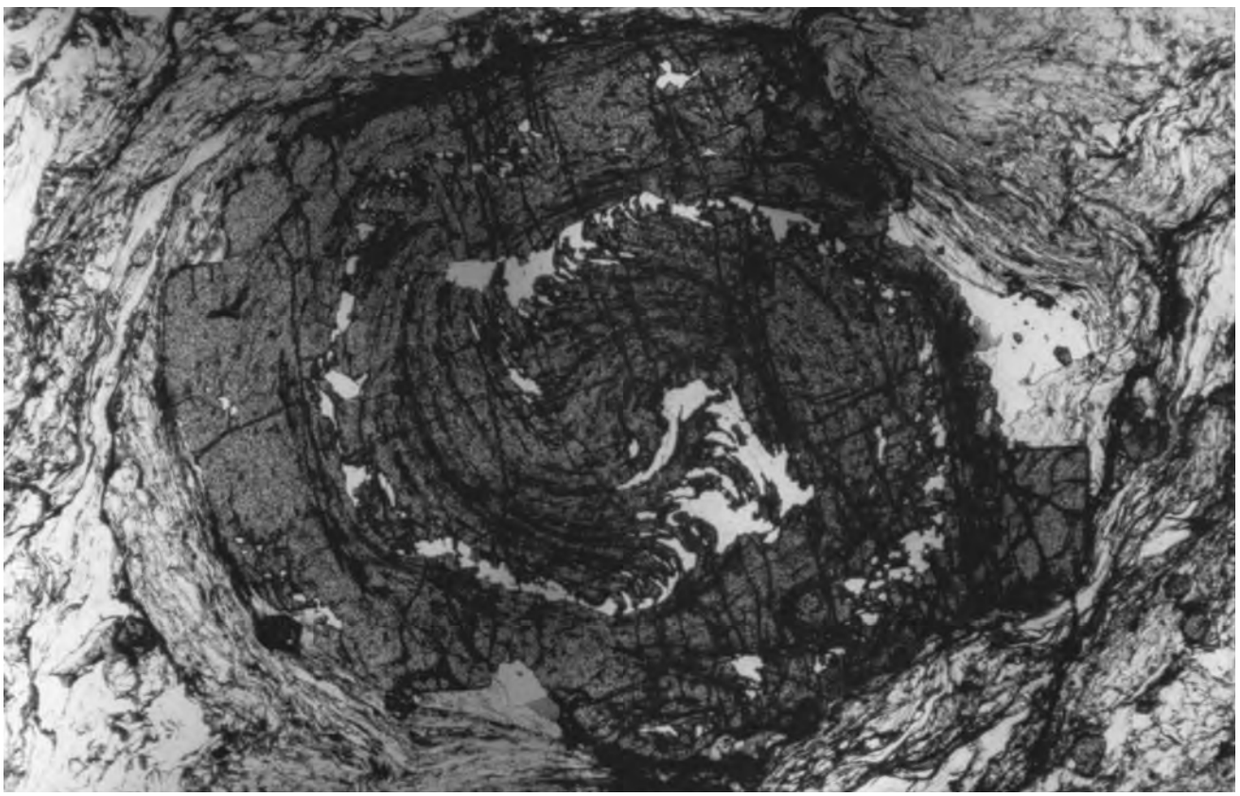

FIGURE 12.13 Snowball garnet (Sweden); width of view is ~7 mm.

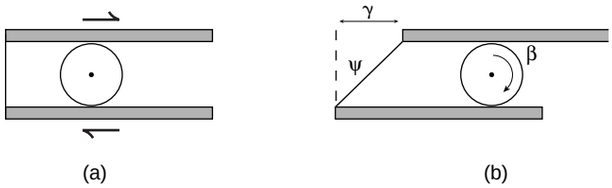

FIGURE 12.14 (a) A simple ball-bearing experiment (b) that illustrates the relationship between rotation (β) and shear (ψ, γ).

ball bearing or a marble between oppositely sliding hands and you will see that its rotation is directly related to the motion of your hands (Figure 12.14). In fact, the amount of rotation of the marble is proportional to the relative displacement of your hands (i.e., the amount of simple shear); mathematically, this relationship is straightforward:

$$\beta = \tan \psi = \gamma \qquad \text{Eq. 12.1}$$

where β is the rotation angle in radians (1 radian is 180°), ψ is the angular shear, and γ is the shear strain (see Chapter 4). However, if the ball bearing is greasy, the rotation angle may be less, because there is some slip between your hands and the ball bearing. This adds to Equation 12.1 a factor that describes the *coupling* between matrix and grain:

$$\beta = \Omega \tan \psi = \Omega \gamma \qquad \text{Eq. 12.2}$$

where the parameter Ω describes the mechanical coupling between the ball bearing and your hands. The value of Ω is equal to 1 for full coupling (clean ball bearing), less than 1 for partial coupling (greasy ball bearing), and 0 for no coupling. In kinematic terms, coupling describes the degree by which internal vorticity is converted to spin. There is no single value for Ω that is unique for natural rocks, but if we assume that grains rotate in a viscous (Newtonian) fluid, considerable slippage will occur at the contact between matrix and grain, and we obtain a theoretical value for Ω of 0.5. Thus, by measuring the rotation angle of the spiraling snowball garnet we can determine the shear strain given some assumption about coupling. Regardless of the coupling assumption, using $\Omega = 1$ gives us an estimate of the minimum shear strain.

12.4.2 Deflected Foliations

Now let's take a closer look at the strain distribution in a shear zone by deforming the middle of three blocks in Figure 12.15 under conditions of non-coaxial strain (simple shear). In Figure 12.15a the strain in the sheared block is homogeneous, because the circles become ellipses with the same axial ratio and orientation. The strain pattern in Figure 12.15b, on the other hand, is heterogeneous as shown by the ellipses of different axial ratio and orientation. Comparing these two patterns with shear zones in a natural rock (e.g., Figure 12.16), we find that inhomogeneous strain dominates. The shear zone in our example is characterized by a mylonitic foliation (S-foliation) that is at ~45° to the shear-zone boundary at the edges of the zone. The S-foliation becomes increasingly parallel to the shear-zone boundary as we approach the center of the zone. If we assume that the trace of the foliation tracks the *X*-axis of the finite strain ellipsoid (Figure 12.17a), the shear strain is determined by the equation

$$\gamma = 2/\tan 2\phi' \qquad \text{Eq. 12.3}$$

where ϕ' is the angle between the foliation and the shear-zone boundary. Note that small differences in the

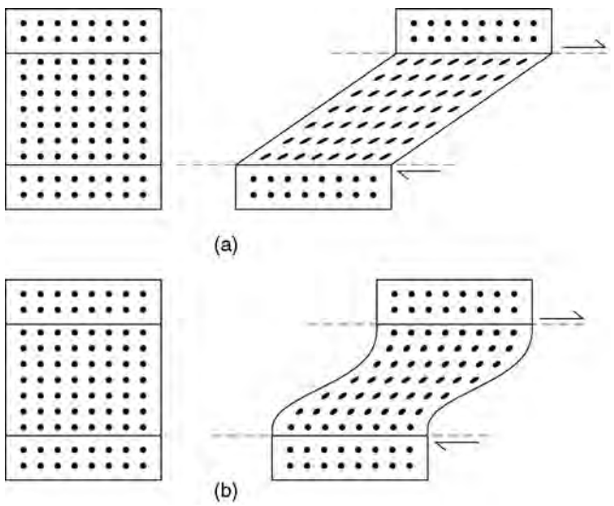

FIGURE 12.15 Homogeneous (a) and heterogeneous (b) strain in shear zones. The similarly shaped and oriented ellipses in (a) show that strain in the zone is homogeneous, whereas variably oriented and elongated ellipses in (b) show heterogeneous strain across the zone.

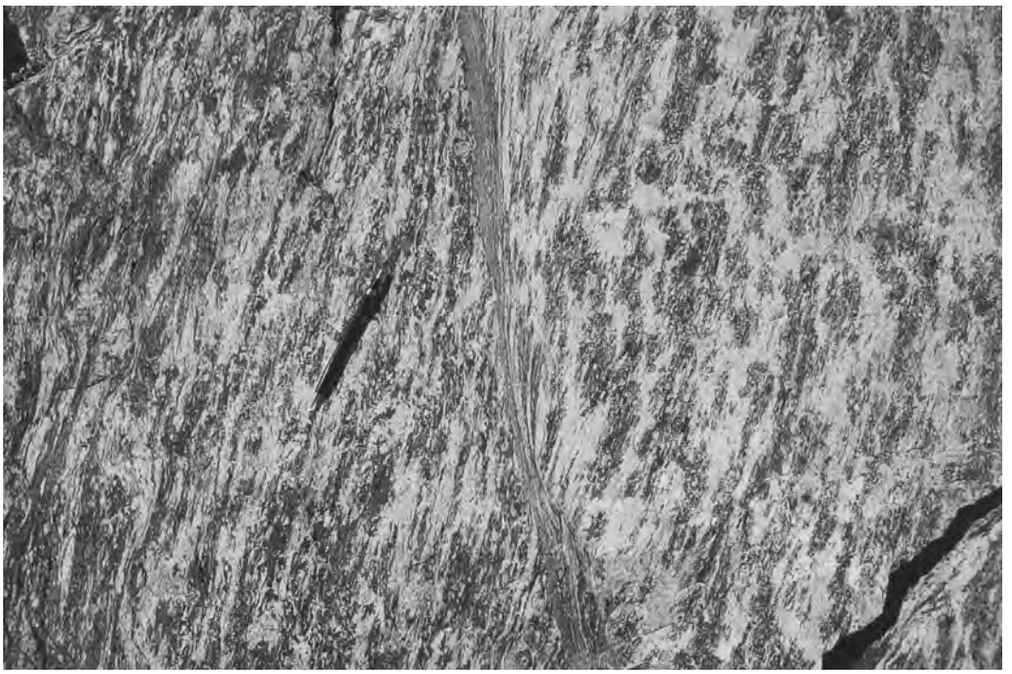

FIGURE 12.16 Small-scale, left-lateral shear zone in anorthosite, showing deflection of the mylonitic foliation (Grenville Orogen, Ontario, Canada). Width of view is ~20cm.

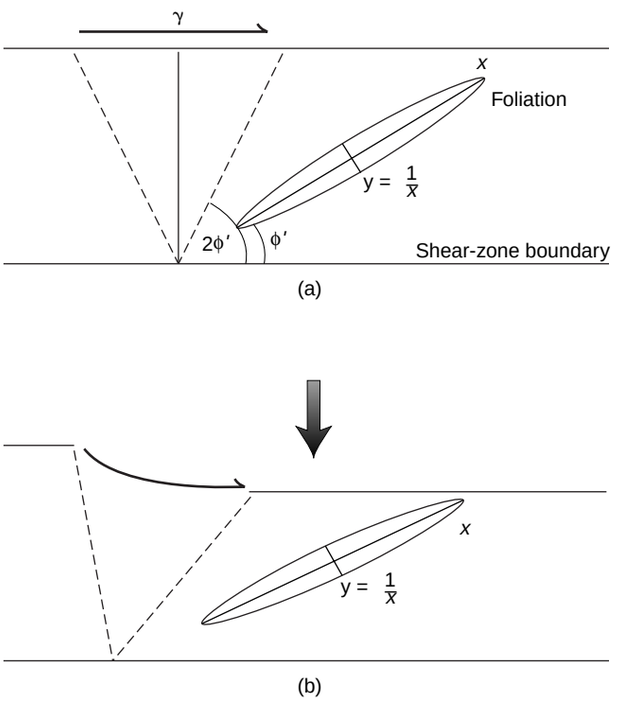

FIGURE 12.17 Angular relationship, ϕ', between foliation and shear-zone boundary, and shear strain, γ, in (a) a perfect shear zone (kinematic vorticity number, W_k, is 1), and in (b) a zone with a component of shortening perpendicular to the shear-zone boundary ($0 < W_k < 1$). Dashed lines are traces of circular sections of the strain ellipse.

value of ϕ' (which occur in the center of the zone) significantly change the calculated magnitude of the shear strain. Just compare the results for ϕ' values of, say, 10° and 5°. Again, in practice, we use this method to obtain a minimum shear strain.

There is yet another issue. Strain determination using Equation 12.3 is more complicated when a component of shortening or extension perpendicular to the shear zone boundary is present (Figure 12.17b); that is, when the strain is nonperfect simple shear (or general shear; Chapter 4). General shear with a shortening component is called **transpression** and with an extensional component is called **transtension.** This pure shear component will change the angle of ϕ', and thus invalidate Equation 12.3, which is based on progressive simple shear. The combination of coaxial and non-coaxial strain cannot be modeled by simply superimposing the two components, because the order of addition matters (recall that tensors are noncommutative). Moreover, simultaneously adding these components produces yet another finite strain, which is shown schematically in Figure 12.18. Deriving the associated equations requires an understanding of strain tensors and matrix operations that is beyond the scope of this book. We leave you simply with the observation that the angle ϕ' will be small even for low shear strains in the presence of a shear zone–perpendicular shortening component and, analogously, the angle may be large with a zone-perpendicular

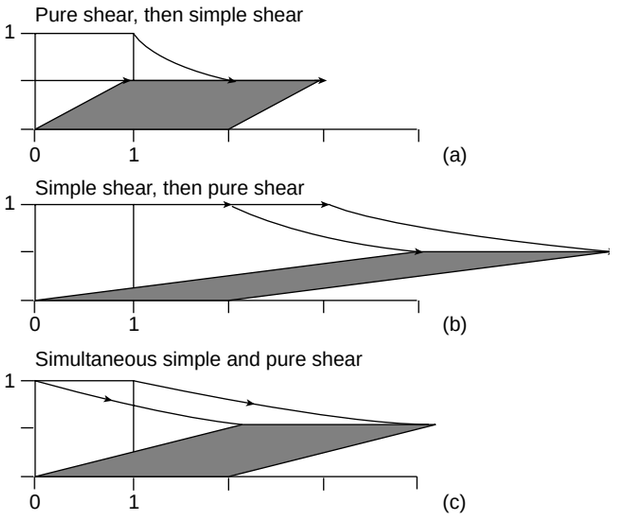

FIGURE 12.18 Comparison of (a) superimposing simple shear on pure shear, (b) superimposing pure shear on simple shear, and (c) simultaneously adding simple and pure shear. The magnitudes of the simple shear and pure shear components are equal in all three examples, but they produce distinctly different finite strains because of the noncommutative nature of tensors.

extensional component. Shear strains obtained from Equation 12.3 will be overestimates and underestimates, respectively, under these conditions. Clearly, strain analysis in shear zones is a complex problem because of the many assumptions it requires, and the results are often rough estimates at best.

12.5 TEXTURES OR CRYSTALLOGRAPHIC-PREFERRED FABRICS

Microstructures describe the geometric relationship between the various constituents of a rock, give an indication of the operative deformation mechanism, and often enable us to form an estimate of the ambient conditions (see Chapter 9). Crystal-plastic deformation mechanisms also provide us with a tool for the interpretation of deformation that is particularly useful in shear zones. Hence we have waited until this point to bring it up. Recall that dislocation glide is the strain-producing crystal-plastic process that occurs on specific crystallographic planes in a crystal (Chapter 9; Table 9.1 lists these glide planes in common rock-forming minerals). The properties of dislocation movement hold the key to interpreting the significance of **textures** or **crystallographic-preferred fabrics** in rocks. It turns out that the type of texture may be indicative of the dominant deformation mechanism and can provide valuable information on the rheologic conditions.

Yet another type of fabric in deformed rocks! You have already learned about dimensional-preferred fabric and now we add crystallographic-preferred fabric to our vocabulary. Let's first see how they differ. Dimensional- and crystallographic-preferred fabrics describe different properties of rocks. A **dimensional-preferred fabric** is the quantification of grain shapes in a rock; it is, in essence, a geometric parameter. Aligned hornblende crystals provide an example of a dimensional-preferred fabric. A **crystallographic-preferred fabric** describes the collective crystallographic orientation of grains that make up the rock. In other words, crystallographic-preferred fabrics represent the degree of alignment of crystallographic axes.

We start by looking at the principles governing the development of crystallographic-preferred orientation by intracrystalline slip. The square *ABCD* in Figure 12.19a marks the schematic cross section of a single crystal that is deformed by homogeneous shortening perpendicular to the top and bottom sides of the square. Stated more specifically, the infinitesimal shortening strain (Z_i) is parallel to *AD* (heavy arrows). The grain only deforms by dislocation glide along specific crystallographic planes, which are shown by the thin lines (parallel to the diagonal *BD*). Let's say that these planes coincide with the basal plane of the crystal with the indices (0001) for hexagonal minerals, so that the crystallographic c-axis is oriented perpendicular to these glide planes. We add one other restriction to the deformation: the faces *AB* and *CD* and the infinitesimal strain axes are held in a constant orientation relative to the external framework, which defines a nonspinning deformation. Because dislocation glide is a volume constant mechanism, the dimensions of the grain measured parallel to the glide plane do not change during deformation. At first glance this may not appear to be the case, but measure the length of the same glide plane in each step (a to c) to prove this to yourself.

During deformation, shortening is accomplished by slip on the glide planes; this is accompanied by simultaneous extension, as shown by the finite strain axis (X_f) in Figure 12.19b. The critical ingredient is that if neither length nor spacing of the glide planes are to change, these planes have to rotate to accommodate the strain. As a consequence, the c-axis (perpendicular to the glide plane) rotates progressively *toward* the infinitesimal shortening direction. Meanwhile, the grain continues to elongate, with the long axis of the finite strain ellipsoid increasingly approaching *AB* (or *CD*). Thus, the finite strain axes and infinitesimal strain axes rotate relative to each other, which defines

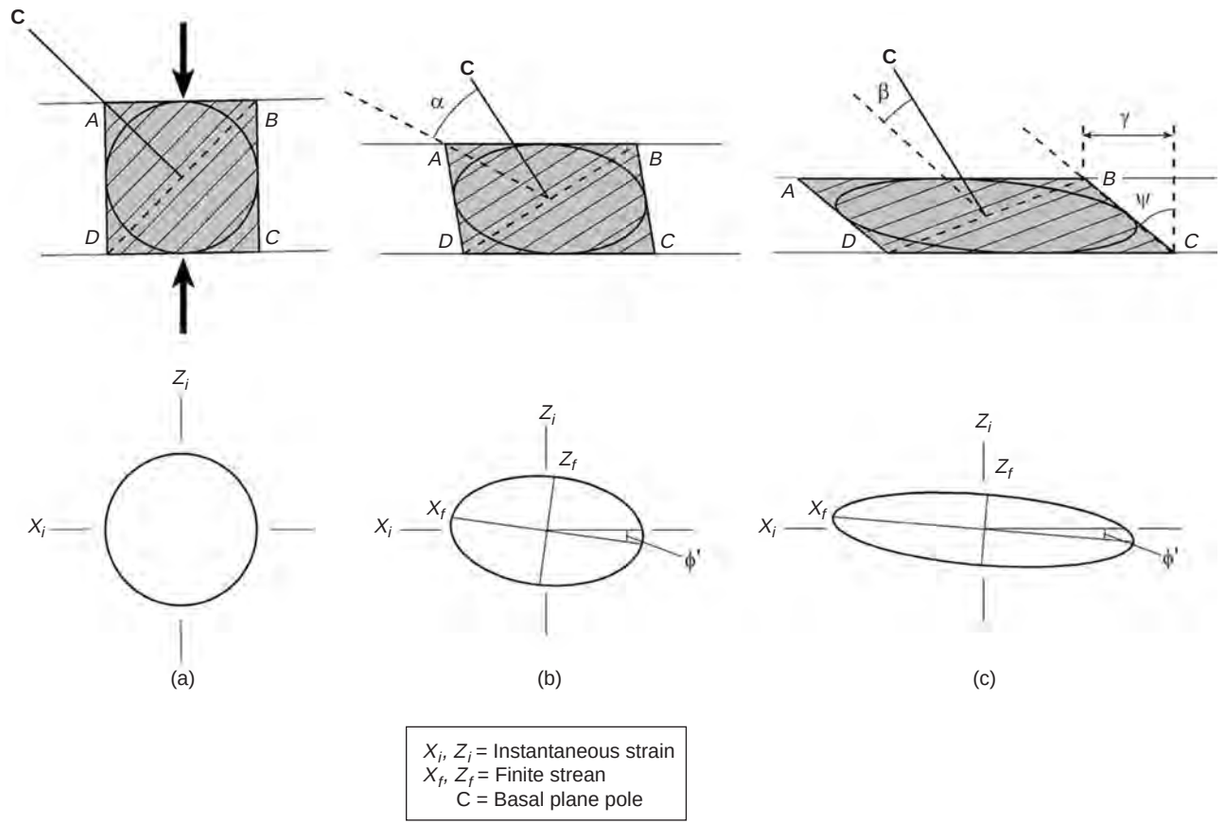

FIGURE 12.19 The development of a crystallographic-preferred orientation by dislocation glide. The thin lines in grain *ABCD* are crystallographic glide planes, which here coincide with the basal plane (0001). The c-axis is indicated with the heavy line, labeled **C,** and the instantaneous shortening direction by heavy arrows. Strain arises from glide on the crystal planes; note that the length of individual planes remains the same, requiring that the glide planes rotate to accommodate the distortion. Various angular relationships are indicated: (α) angle of shear along the glide plane; (β) rotation angle of the c-axis with respect to an external reference system (e.g., shear-zone boundary); (ψ) rotation angle of material line *BC* with respect to an external reference system (angular shear); (ϕ') angle of finite extension axis (subscript "*f*") with respect to an external reference system. Note that the instantaneous strain axes (subscript "*i*") define the external reference system, and that they do not change in orientation during the progressive history (i.e., there is no spin).

non-coaxial strain with simultaneous nonspinning deformation. In this generalized scenario, we recognize two important consequences: (1) the c-axes rotate toward the instantaneous shortening axis (Z_i) and (b) the finite strain ellipsoid elongates toward the instantaneous shortening direction (X_i), which means that they are only parallel at very large strains. In Nature, matters may be more complex as we are dealing with three-dimensional space in which several glide planes may be active simultaneously. Computer modeling of the development of crystallographic fabrics in these more complex situations, however, shows overall behavior similar to that in our simple model. We can use these characteristics of texture development for the determination of shear sense, but, for this, we first must be familiar with the Symmetry Principle.

12.5.1 The Symmetry Principle

Symmetry is a common and fascinating aspect of the world around us. Look in the mirror or at your neighbor and you see that a person's face is symmetric (at least in general) around a single plane. This symmetry plane cuts between the eyes, and divides the nose and mouth in halves (bilateral or mirror symmetry). Most objects, living or inanimate, display some degree of symmetry, as do many of the geometric concepts basic to mathematics and physics. A cube has a higher symmetry than the human face, in that it contains three mutually perpendicular **mirror planes.** We say that a cube has a higher symmetry than a human face, because it contains more symmetry elements. In mineralogy, you have learned about the symmetry of various types of crystals; for example, triclinic (only a center of symmetry or a two-fold axis),

TABLE 12.3 CRYSTAL SYSTEMS IN ORDER OF INCREASING SYMMETRY

System	Symmetry	Crystal Axes[1]
Triclinic	1 one-fold axis or center of symmetry	$a \neq b \neq c$, $\alpha \neq \beta \neq \gamma \neq 90°$
Monoclinic	1 two-fold axis or 1 symmetry plane	$a \neq b \neq c$, $\alpha = \gamma = 90°$, $\beta \neq 90°$
Orthorhombic	3 two-fold axes or 3 symmetry planes	$a \neq b \neq c$, $\alpha = \beta = \gamma = 90°$

[1]a, b, and c describe the lengths of the crystal axes; α is the angle between b and c; β is the angle between a and c; γ is the angle between a and b.

monoclinic (one mirror plane), and orthorhombic (three mutually perpendicular planes with intersections of unequal length). Any introductory mineralogy textbook will refresh your memory on crystal symmetry and in Table 12.3 we list the characteristics of these systems that are most pertinent to our discussion.

Let's explore the **Symmetry Principle** (or Curie principle[5]) with a simple example (Figure 12.20). Imagine that we apply strain to a cube such that the resulting shape is a rectangular block. The symmetry of the rectangular block is orthorhombic (three perpendicular symmetry planes or three perpendicular two-fold axes; Figure 12.20a). The symmetry of the simplest strain path causing this shape change is also orthorhombic, meaning that the incremental and finite strain ellipsoids differ only in shape, not in orientation (i.e., coaxial strain). We restate this by distinguishing the cause (the strain path) and the effect (the rectangular block): the effect has a symmetry that is equal to or greater than the cause. This is called the Symmetry Principle. Now we distort our cube, say by shear, such that it becomes a block with a lower symmetry (Figure 12.20b). In this case the resulting symmetry is monoclinic, because we can only recognize one mirror plane and one two-fold axis. Using the Symmetry Principle we therefore predict that the strain path (meaning, the cause) must have monoclinic or lower symmetry. Thus, the strain that caused the distortion must have been non-coaxial, as coaxial strain would have produced higher symmetry.

If the Symmetry Principle says that the effect is of equal or greater symmetry than the cause, is the reverse also true? No, the cause cannot have a symmetry that is

[5]After the French scientist Pierre Curie (1859–1906).

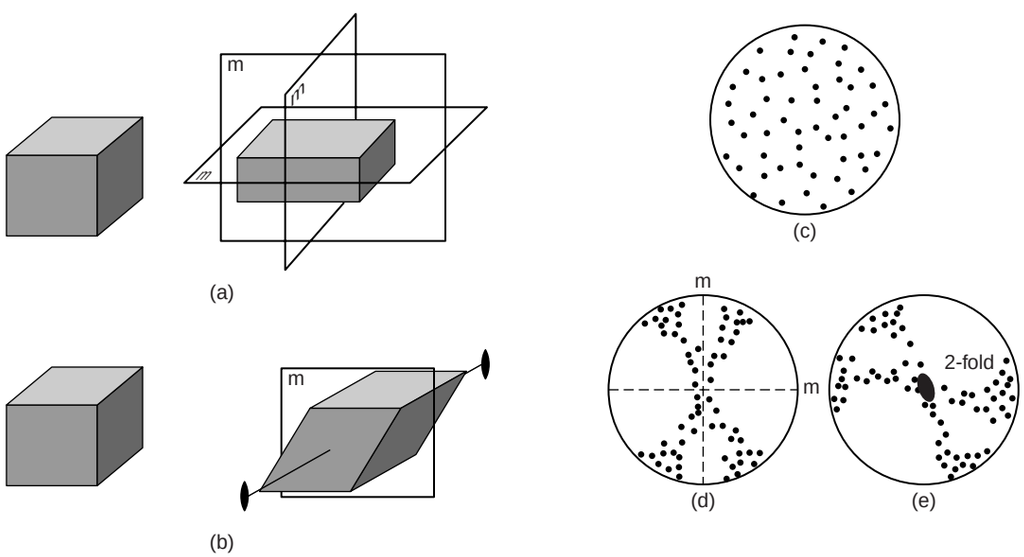

FIGURE 12.20 The Symmetry Principle. A cube is distorted into a body with (a) orthorhombic and (b) monoclinic symmetry. (c) A random distribution of c-axis pattern reorganizes in response to these deformations into (d) a high-symmetry (orthorhombic) and (e) a low-symmetry (monoclinic) pattern. The symmetry of the c-axes patterns enables us to predict the strain path.

higher than the effect. This is all fine and good, but what does it have to do with crystallographic-preferred fabrics? Figure 12.20c shows a random pattern of crystallographic c-axes in lower hemisphere projection, say from a statically recrystallized quartzite. In two separate deformation experiments we form characteristic c-axis patterns (Figure 12.20d and e). The symmetry of the two patterns is different; the pattern in Figure 12.20d has orthorhombic symmetry, whereas the pattern in Figure 12.20e is monoclinic. What can we say about the strain that produced these crystallographic patterns? Using the Symmetry Principle, the pattern in Figure 12.20d must have been caused by a strain path with a symmetry equal to or less than orthorhombic, whereas the symmetry of the strain path that produced the pattern in Figure 12.20e must have been monoclinic or lower. Thus, Figure 12.20e ("the effect") can only have been formed by non-coaxial strain ("the cause"). Note that the pattern in Figure 12.20d, however, cannot be uniquely interpreted; it could have formed by either coaxial or non-coaxial strain according to the Symmetry Principle. With this information we can use textures to indicate whether the rocks were deformed in a non-coaxial or coaxial strain regime. Perhaps more importantly, the Symmetry Principle provides a means to determine shear sense in rocks.

12.5.2 Textures as Shear-Sense Indicators

Imagine an aggregate of grains that each slip on the same single glide plane, but that initially is randomly oriented in our sample (Figure 12.21). This situation is slightly more complex than our previous single-grain condition (Figure 12.19), because neighboring grains will affect the ability of grains to slip.[6] When shearing the aggregate, a pattern emerges in which the majority of c-axes rotate toward an orientation perpendicular to

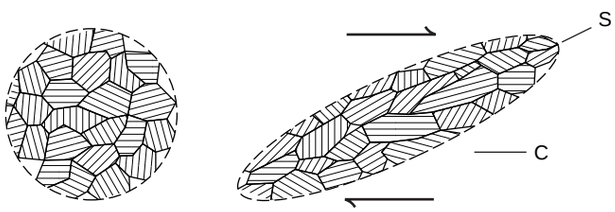

FIGURE 12.21 The relationship between shape, crystallographic fabric, mylonitic foliation (S) and shear plane (C) in a grain aggregate with a single operative glide plane for each grain.

[6]This is called the *compatibility problem.*

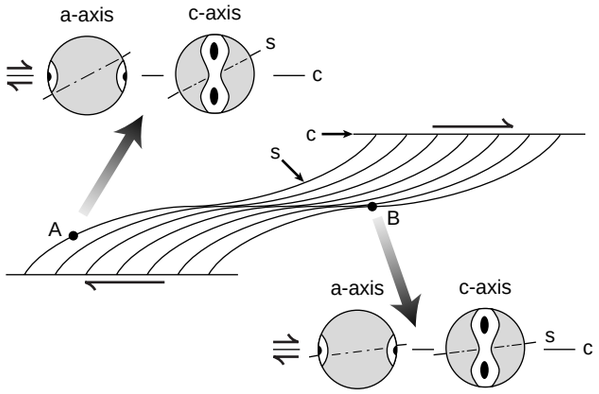

FIGURE 12.22 Schematic illustration of foliation in shear zone and associated crystallographic fabrics. The angular relationship between S and C decreases with increasing shear strain (as recorded by S-foliation deflection), producing characteristic c-axis patterns (compare regions A and B). The corresponding a-axis patterns show no change.

the bulk shear plane (C in Figure 12.21). At the same time a dimensional-preferred fabric is formed that defines the mylonitic foliation (S-foliation), which is oblique to the shear zone boundary (C-surface). Thus, the c-axis fabric is oblique to the S-foliation in a sense similar to that of the shear sense in the zone (region A in Figure 12.22); in other words, the c-axis girdle tilts in the direction of shear. With increasing shear, the obliquity is less because the S and C surfaces approach parallelism, which means that in the center of the shear zone the interpretation of textures is restricted (region B in Figure 12.22). The solution to this situation is measurement of a traverse across the shear zone.

The natural c-axis fabric for quartz shown in Figure 12.23b is consistent with our model. But is this pattern a rule that can be applied to all minerals? Unfortunately, the answer is no. Look at the calcite c-axis fabric (Figure 12.23a), in which slip occurred on

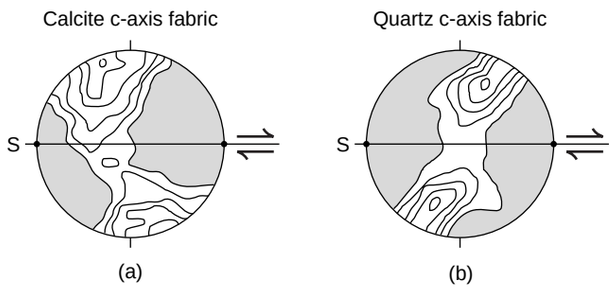

FIGURE 12.23 Asymmetric c-axis fabrics for (a) calcite and (b) quartz from natural shear zones, showing contrasting patterns resulting from the operation of different glide planes. In quartz, basal slip occurred, whereas e-twinning dominated calcite deformation. Note that the mylonitic foliation (S) is used for reference (compare with Figure 12.22).

the e-plane of calcite (calcite twinning; Table 9.1). The displacement is again right-lateral, but here the c-axes lie in the opposite quadrant from those of the quartz fabric in Figure 12.23b. This is not a paradox, but reflects the operative slip system. Quartz deformed predominantly by slip on the basal plane [(0001)-plane], whereas calcite slip occurred by e-twinning. Calcite crystallographic fabrics that are formed by slip on other glide planes will, in fact, produce c-axis patterns that are similar to that for quartz. These observations from natural rocks highlight the importance of knowing the operative slip system before crystallographic patterns can be used as a shear-sense indicator. Determining these patterns requires complementary electron microscopy and measuring the orientation of other crystallographic axes in the same sample (such as the a-axis; Figure 12.22).

The measurement of crystallographic fabrics requires careful preparation of oriented thin sections and tedious measurement of crystallographic orientations with an optical microscope that is equipped with a universal stage or optical sensors. Other techniques, such as scanning electron microscopy, and X-ray and neutron-source methods, are rapidly becoming available for more automated analysis. Crystallographic fabric analysis is most commonly applied to monomineralic rocks consisting of relatively simple minerals such as quartz, calcite, and olivine, but more complex minerals, such as feldspar, can also be studied. For each grain the orientation of a particular crystallographic axis is measured and plotted in spherical projection. Typically, the orientation of the mylonitic foliation (S) or the shear zone boundary (C) is taken as E-W (East–West) and vertical; it is critical for the interpretations to label these foliations carefully (recall their relationship as a function of shear sense; see Figure 12.11). A reliable crystallographic-preferred fabric measurement involves at least 100–150 grains. A crude estimate of the degree of crystallographic-preferred orientation may be obtained with the optical microscope by inserting the gypsum plate (1/4-wavelength) under crossed polarizers and slowly rotating the sample. If there is an obvious fabric, the color of most grains will change at the same time; for example, from blue to yellow in quartz. Otherwise, you will see an irregular pattern of colors that is a mix of red (the extinction color), yellow, and blue.

A final note: Crystallographic fabrics mainly reflect the *latest stages* of the deformation history, because recrystallization processes tend to erase the early history. Nonetheless, crystallographic fabrics offer a valuable tool to unravel the deformation history of rocks and regions, as you will see by looking at the modern structural geology literature.

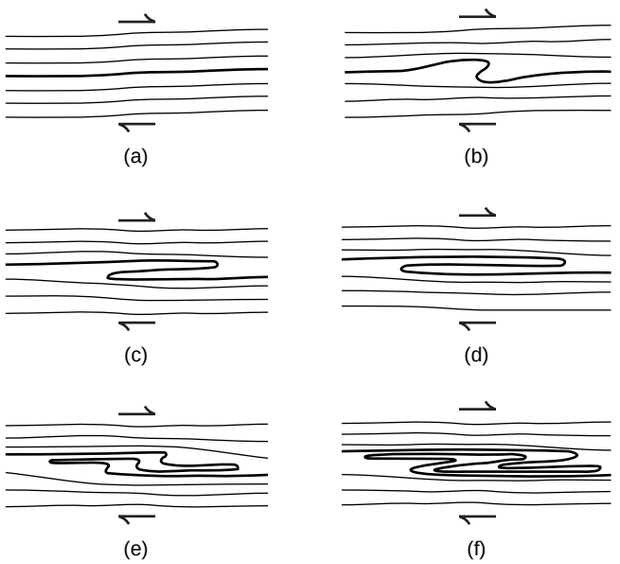

FIGURE 12.24 Fold transposition in a layered rock that undergoes non-coaxial, layer-parallel displacement. An asymmetric fold develops at a perturbation (a–d), which in turn gets refolded (e–f). The end result is a superimposed fold structure that is essentially parallel to the dominant layering. Note that if the second fold had formed at another location, the two would have been indistinguishable, although formed at different times.

12.6 FOLD TRANSPOSITION

At first glance, folds appear to be less common in ductile shear zones than one would expect; but upon closer inspection they are found to occur with a peculiar appearance. In Figure 12.24 an asymmetric fold is formed from a small instability by foliation-parallel shear. With increasing shear, the oblique (short) limb of the asymmetric fold rotates back into a foliation-parallel orientation (Figure 12.24a–d). The resulting perturbation gives rise to a new fold that is superimposed on the original structure. Continued shear reorients the fold pattern back into a layer-parallel orientation (Figure 12.24e–f), leaving behind a complex geometry that can only be interpreted by carefully tracing the layering (Figure 12.25). This scenario, called **fold transposition,**[7] highlights two aspects of folds in shear zones. (1) Fold asymmetry may be representative for the sense of shear; that is, Z-vergence occurs in right-lateral shear zones while S-vergence occurs in left-lateral shear zones. We state this only as a possibility and not as a rule, because at high shear strains the vergence of small folds may actually reverse

[7]Originally described as "Umfaltung" by the early-twentieth-century German geologist Bruno Sander, who pioneered modern structural analysis.

(a)

(b)

FIGURE 12.25 Transposed mafic layer in a granitic gneiss (Grenville Orogen, Ontario, Canada). The mafic (dark) layer can be traced as a single bed that is refolded numerous times in the outcrop (a). A detail of the large structure, which is affectionately known as the "snake outcrop," highlights the complexity of folding; person for scale.

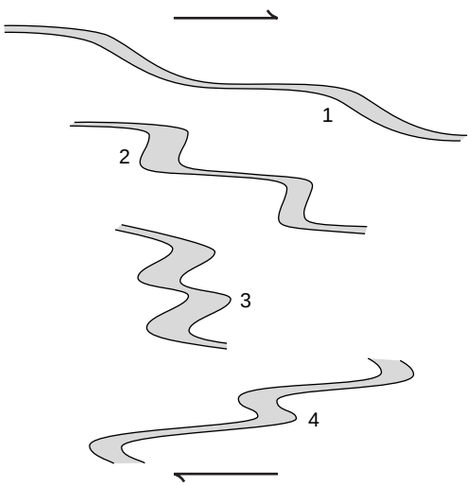

FIGURE 12.26 Schematic illustration of reversal in fold vergence (from "S-shape" to "Z-shape"), with increasing shear strain in a right-lateral shear zone.

(Figure 12.26). (2) Folding is a progressive process, resulting in complex patterns of folding and refolding. Fold transposition occurs at all scales, from microfolds to kilometer-scale folds, and is, in fact, not restricted to zones of non-coaxial strain.

Folds in areas of high strain are often disrupted, preserving only isolated fold hinges or fold hooks (so called because of their resemblance to fishing hooks). Consider shortening that occurs parallel to competent layers in a less competent matrix, say sandstone layers in a shale matrix. The result is folds with an upright axial surface (Figure 12.27a); the **fold enveloping surface** is drawn for reference. Progressive shortening produces thinning of limbs and, locally, hinges become detached (Figure 12.27b; a natural example of this stage is shown in 12.27d). Eventually, we are left with a rock texture that is characterized by a single layering with lenses of more competent material (Figure 12.27c). Without knowledge of the history, the fabric in Figure 12.27c shows little or no indication of the original geometry, especially if the structures are very large (say kilometers). A cursory examination would suggest that overall bedding is updown, until you notice the presence of the small fold hooks and maybe minor isoclinal folds. Only then do you realize that fold transposition has occurred. Transposed fabrics are even more pronounced when an axial-plane foliation is formed, which will be nearly parallel to transposed layering (Figure 12.27c). As a consequence, pretty much all layering in the rock seems parallel, with the exception of preserved fold hinges. Transposition in non-coaxial shear zones similarly results in a geometry in which all layering is roughly parallel to the shear-zone boundary. Try to sketch the evolution of folds in a non-coaxial environment, using Figure 12.26 as a starting point, and track the orientation of the enveloping surface for comparison with the coaxial strain scenario in Figure 12.27.

Rather than being the exception, transposition is more likely the rule in deformed metamorphic areas, where it is promoted by the overall weakness of layers at elevated pressures and temperatures (such as the rocks in Figure 12.25). In addition to unraveling the deformation history, identifying transposition is important if you wish to erect a regional stratigraphy for an area, because it poses the question of whether repetition of a particular lithology is primary or structural in origin. So, are there *criteria* to recognize transposition? One clue is a regular repetition of lithologies; for example, repeated marble layers in an area of mafic gneisses may, on a regional scale, outline large transposed folds. When a sequence of lithologies exists, say gabbro-gneiss-marble, its repetition in reversing order is suggestive of transposition. Parallelism between foliation and bedding is not diagnostic by itself, but it should

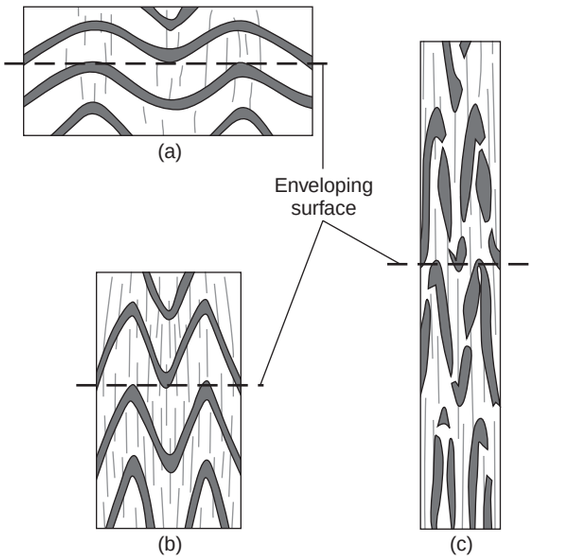

(d)

FIGURE 12.27 Fold transposition. Progressive coaxial strain (a–c) results in isoclinal folds that become disrupted by limb attenuation and boudinage. The fold enveloping surface is shown for reference. (d) A natural example of an early stage of transposition (Newfoundland, Canada); pencil for scale.

make you suspicious. The occurrence of minor isoclinal folds and fold hooks (especially if the foliation is axial-planar to these structures) adds weight to the case. You wrap it up by showing reversals in the direction of younging in layers across the area changes. Unfortunately, younging evidence is hard to find in medium- to high-grade metamorphic areas, but in low-grade metamorphic areas (greenschist facies and down) the observant geologist often finds evidence for younging. Your efforts to prove a case of transposition will bear fruit. Transposition results in a radical reinterpretation of stratigraphic relationships by showing that "stratigraphy" in the area is, in fact, structural in origin, and that the real stratigraphy is simpler. Secondly, a previously unrecognized early stage of isoclinal folding has major implications for the structural evolution of the area. In the section on regional geology (Chapters 21 and 22) you will see that exhumed rocks in many mountain belts show early stages of large-scale isoclinal folding, typically associated with thrusting, which is manifested in outcrop by fold transposition.

12.6.1 Sheath Folds

In closing this chapter, we describe one particular type of fold that is restricted to regions of high shear: **sheath folds.** In contrast to the ambiguity of fold vergence in shear zones already described (Figure 12.26), sheath folds can define shear-sense in ductile shear zones. They are typically exposed as eye-shaped outcrop patterns that represent a section through the nose of the fold (Figure 12.28). Sheath folds are a special type of doubly plunging folds (see Chapter 10), where the hinge line is bent around by as much as 180°. In other words, layering in a sheath fold is everywhere at a high angle to the profile plane, which gives the characteristic eye-shaped outcrop pattern. Sheath folds are formed when the hinge line of a fold rotates passively into the direction of shear, while the axial surface rotates toward the shear plane (Figure 12.29a). Note that sheath folds differ from "dome-and-basin" type fold interference patterns, because they form by progressive strain under the same overall deformation regime, rather than reflecting two discrete deformation regimes (see superposed folding; Section 10.6.2). Since hinge rotations require high amounts of shear strain, the occurrence of sheath folds is limited to ductile shear zones. The degree of hinge rotation is a function of shear strain and the angular relationship of hinge line with the shear plane. However, sheath folds cannot be used as a strain gauge beyond the general comment of "large amount of shear," unless these initial angular relationships are known.

The location of the nose of sheath folds points in the direction of movement, but this can be determined only when the folds are fully exposed (including the nose!). In less-rotated portions of a sheath fold, the shear sense may also be derived from hinge line rotation (Figure 12.29a).[8] Most commonly, sheath folds define the direction of shear rather than shear sense, with the hinge line approximately parallel to the shear direction.

12.7 CLOSING REMARKS

It is fairly certain that you will encounter shear zones (and transposition) on a field trip or in your study area; you may already have done so. There is no better way to learn about the variety of deformation

[8]Similar to the Hansen slip line method.

FIGURE 12.28 A sheath fold in amphibolite gneiss showing the characteristic eye-shaped outcrop pattern (Grenville Orogen, Ontario, Canada); hammer for scale.

features in shear zones than by direct observation. In many instances you will be unable to convince yourself of important concepts, such as sense of shear or "stratigraphy," unless you allow ample time for outcrop examination. As a rule, it is more useful to understand one outcrop well, than many outcrops in a cursory fashion; one single outcrop may, in fact, hold the key to the interpretation of an entire area. Unfortunately, it is another rule that this special outcrop is invariably to be found in the most remote part of the area, on the highest peak, and on the rainiest day. Until you find that Rosetta Stone[9] of structural analysis, any well-studied outcrop offers you a working hypothesis that can be tested in other places. Only later, after many outcrops, will you learn which of them is your area's "Rosetta Stone."

Once mylonitization begins (protomylonite stage), the resulting microstructures further weaken the zone relative to the host rock. Thus, strain will continue to be localized in a zone and the mylonite will evolve. A variety of potential shear-sense indicators are

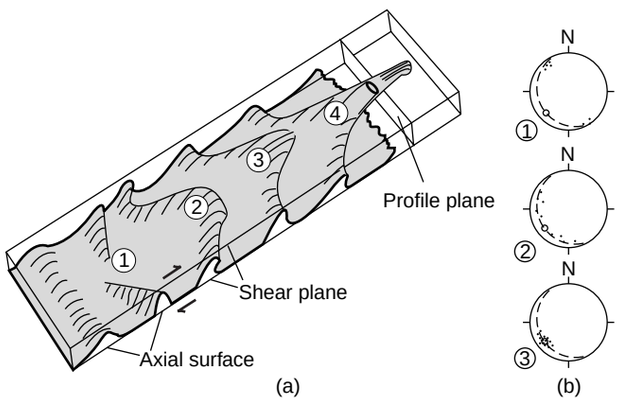

FIGURE 12.29 Sheath folds are formed when weakly doubly-plunging folds are modified in a zone of high shear strain. Several stages of fold modification occur, with the most evolved stage producing the characteristic conical geometry of a sheath fold (fold 4). The progression in (a) has the lowest amount of shear at the left and the highest shear strain at the right. Note the progressive curvature of the hinge line in folds 1 to 3, which typically is accompanied by a (stretching) lineation in outcrop. In (b), the corresponding lower-hemisphere projections of hinge lines in folds 1, 2, and 3 are shown. The great circle represents the shear plane and the open circle the shear direction; small dots are hinge-line measurements. When fully exposed, sheath folds can be used as a shear-sense indicator with the nose pointing in the direction of transport; otherwise, sheath folds indicate the direction of shear only.

[9]This slab of basalt, discovered in the late eighteenth century, enabled linguists to decipher Egyptian hieroglyphs because it contained the same text in three languages, one of which was Greek.

available for ductile shear zones, but their kinematic significance is not fully understood. Most of these indicators are based on empirical observations, and one should not interpret shear sense based on a single indicator in one location only, no matter how classic an example it is. Reliable predictions are based on several independent indicators, which each support the same shear sense. Even then, caution should be exercised with tectonic interpretations, because a shear zone may be subsidiary to a larger system, so that the shear sense is only representative of the zone in question (remember the analogous situation with changing fold vergence in a large fold; Section 10.4.2). After addressing all caveats, you will find that ductile shears will deliver on their promise. To end this sequence of chapters on ductile deformation, we close with some tools from related Earth science disciplines that further aid the modern structural geologist in unraveling the history of deformed rocks and regions.

ADDITIONAL READING

Fossen, H., and Tikoff, B., 1993. The deformation matrix for simultaneous simple shearing, pure shearing and volume change, and its application to transpression and transtension tectonics. *Journal of Structural Geology,* 15, 413–422.

Hanmer, S., and Passchier, C., 1991. Shear-sense indicators: a review. *Geological Survey of Canada,* Paper 90–17, 72 pp.

Law, R. D., 1990. Crystallographic fabrics: a selective review of their applications to research in structural geology. In Knipe, R. J., and Rutter, E. H., eds., *Deformation mechanisms, rheology and tectonics. Geological Society Special Publication,* 54, 335–352.

Lister, G. S., and Snoke, A. W., 1984. S-C mylonites. *Journal of Structural Geology,* 6, 617–638.

Passchier, C. W., and Simpson, C., 1986. Porphyroclast systems as kinematic indicators. *Journal of Structural Geology,* 8, 831–843.

Ramsay, J. G., and Graham, R. H., 1970. Strain variation in shear belts. *Canadian Journal of Earth Sciences,* 7, 786–813.

Ramsay, J. G., and Huber, M. I., 1983/1987. *The techniques of modern structural geology, volumes 1 and 2.* Academic Press, 700 pp.

Sibson, R. H., 1977. Fault rocks and fault mechanisms. *Journal of the Geological Society of London,* 133, 191–213.

Simpson, C., 1986. Determination of movement sense in mylonites. *Journal of Geological Education,* 34, 246–261.

Simpson, C., and De Paor, D. G., 1993. Strain and kinematic analysis in general shear zones. *Journal of Structural Geology,* 15, 1–20.